A Network Flow Method for Improved MR Field Map Estimation in the Presence of Water and Fat

D. Hernando, P. Kellman, J. P. Haldar and Z.-P. Liang

***Abstract*— Field map estimation is an important problem in MRI, with applications such as water/fat separation and correction of fast acquisitions. However, it constitutes a nonlinear and severely ill-posed problem requiring regularization. In this paper, we introduce an improved method for regularized field map estimation, based on a statistically motivated formulation, as well as a novel algorithm for the solution of the corresponding optimization problem using a network flow approach.**

The proposed method provides theoretical guarantees (local optimality with respect to a large move), as well as an efficient implementation. It has been applied to the water/fat separation problem and tested on a number of challenging datasets, showing high-quality results.

I. Introduction

In MRI, a very homogeneous main (B_0) magnetic field is desirable. However, inhomogeneities in the B_0 field are often unavoidable, due to susceptibility differences introduced by the object being imaged, as well as magnet imperfections. These inhomogeneities introduce undesired, spatially-varying phase shifts in the MR signal, which can be corrected given knowledge of the true B_0 field. Hence, estimation of the B_0 field inhomogeneity map (or "field map") is an important problem in MRI, as it allows, e.g., effective water/fat separation, correction of EPI/spiral acquisitions, and automated shimming [1]–[3].

The field map can be estimated based on the phase evolution of a sequence of images acquired at different echo times, $t_1, t_2, \ldots, t_N$. In this work, we consider the presence of signal originating from water and fat, which further complicates the problem, as these two components have different phase behavior [4]. The signal at an individual voxel q can therefore be modeled as:

$$s_q(t_n) = e^{i2\pi f_{\text{B}} t_n} \left(\rho_{\text{W}} + \rho_{\text{F}} e^{i2\pi f_{\text{F}} t_n} \right) \tag{1}$$

where t_n is the echo time shift, f_{B} (in Hz) is the local frequency shift due to B_0 field inhomogeneity, ρ_{W} and ρ_{F} are the intensities of the water and fat components, respectively, and f_{F} (in Hz) is the frequency shift of fat, which is assumed known *a priori*.

Field map estimation is a difficult problem due to the nonlinearity of the signal model and the presence of phase wraps (particularly in cases of high field inhomogeneity). To alleviate these problems, the estimated field map is typically regularized by imposing spatial smoothness. Most previously proposed methods resort to a two-step approach for estimating the regularized field map: first, f_{B} is estimated voxel-by-voxel using a maximum-likelihood (ML) criterion, and second, the resulting (noisy) field map is low-pass filtered to achieve the desired smoothness [5]. The main drawback of this method is that, while the low-pass filtering is generally effective in removing small noise-related perturbations in the field map, it is unable to correct the large errors due to the ill-posedness of the voxel-by-voxel estimation problem. Several extensions have been proposed to improve the initial voxel-by-voxel estimation [6]. In Ref. [7], a method is developed for directly estimating the regularized field map, assuming the presence of only water (i.e., $\rho_{\text{F}} = 0$ in Eq. 1). This method formulates the estimation as a penalized ML (PML) problem, which is solved iteratively using conjugate gradients, producing a locally optimal solution.

In this paper, we introduce a novel method for regularized field map estimation in the presence of water and fat, based on a PML formulation and an improved iterative optimization algorithm consisting on mapping each step to an equivalent network flow problem on a suitable graph.

II. Methods

A. Problem formulation

The signal model in Eq. 1 contains three unknown parameters: $\{\rho_{\text{W}}, \rho_{\text{F}}, f_{\text{B}}\}$. Under the assumption of white additive Gaussian noise, the ML estimate for $\{\rho_{\text{W}}, \rho_{\text{F}}, f_{\text{B}}\}$ is obtained by minimizing the following cost function at each voxel q:

$$R_0(\rho_{\text{W}}, \rho_{\text{F}}, f_{\text{B}}; \mathbf{s_q}) = \sum_{n=1}^{N} \left| s_q(t_n) - e^{i2\pi f_{\text{B}} t_n} \left(\rho_{\text{W}} + \rho_{\text{F}} e^{i2\pi f_{\text{F}} t_n} \right) \right|^2 \tag{2}$$

where N is the number of different echo times employed (typically $N = 3$), $s_q(t_n)$ is the measured signal at voxel q and echo time t_n, and $\mathbf{s_q} = [s_q(t_1) \cdots s_q(t_N)]^T$.

Minimizing $R_0(\rho_{\text{W}}, \rho_{\text{F}}, f_{\text{B}}; \mathbf{s_q})$ is a separable nonlinear least-squares (NLLS) problem. As shown in [8], estimation of f_{B} can be isolated using the variable projection (VARPRO) formulation, reducing to the minimization of:

$$R(f_{\text{B}}; \mathbf{s_q}) = \left\| \left[\mathbf{I} - \mathbf{\Psi}(f_{\text{B}}) \mathbf{\Psi}^{\dagger}(f_{\text{B}}) \right] \mathbf{s_q} \right\|_2^2 \tag{3}$$

This work was supported in part by the following research grants: NIH-P41-EB03631-16 and NIH-R01-CA098717.

D. Hernando, J. P. Haldar and Z.-P. Liang are with the Department of Electrical and Computer Engineering, University of Illinois at Urbana-Champaign, Urbana, IL 61801, USA {dhernan2, haldar, z-liang} @uiuc.edu

P. Kellman is with the Laboratory of Cardiac Energetics, National Heart, Lung and Blood Institute, National Institutes of Health, Department of Health and Human Services, Bethesda, MD 20892, USA kellmanp@nhlbi.nih.gov

where

$$\Psi(f_{\rm B}) = \begin{pmatrix} e^{i2\pi f_{\rm B} t_1} & e^{i2\pi (f_{\rm F}+f_{\rm B}) t_1} \\ e^{i2\pi f_{\rm B} t_2} & e^{i2\pi (f_{\rm F}+f_{\rm B}) t_2} \\ \vdots & \vdots \\ e^{i2\pi f_{\rm B} t_N} & e^{i2\pi (f_{\rm F}+f_{\rm B}) t_N} \end{pmatrix} \tag{4}$$

(see [8] for details).

The residual R is a nonconvex function of $f_{\rm B}$, and typically contains multiple local minima. As shown in Ref. [8], evaluating R on a grid containing L uniformly spaced field map values, $\Omega = \{f_{\rm MIN} + l\Delta f\}_{l=1}^{L}$, allows us to overcome this nonconvexity (since we can simply pick the minimizer). However, voxel-by-voxel field map estimation is generally still an ill-posed problem, as shown in Fig. 1, where R has multiple global minimizers (note that R is actually periodic for acquisitions with uniformly spaced echo times). In addition, the presence of noise may yield nonsmooth field map estimates, which is often undesirable. To address both of these issues, we adopt a PML approach combining R with a spatial smoothness term, which can be viewed as imposing a Markov Random Field (MRF) prior on the field map [9]. In this framework, estimation of the complete field map $\mathbf{f}_{\rm B} = [f_{{\rm B},1}\ ,\ f_{{\rm B},2}\ , \cdots ,\ f_{{\rm B},Q}]$ (where Q is the number of voxels in the image) reduces to the following discrete optimization problem:

$$\hat{\mathbf{f}}_{\rm B} = \arg \min_{\{f_{{\rm B},q}\in\Omega\}_{q=1}^{Q}} \sum_{q=1}^{Q} R(f_{{\rm B},q};\mathbf{s_q}) + \mu \sum_{q=1}^{Q} \sum_{j\in\delta_q} w_{q,j} V(f_{{\rm B},q}, f_{{\rm B},j}) \tag{5}$$

where δ_q is the MRF neighborhood of voxel q, μ is a regularization parameter balancing data consistency and smoothness of the solution, $w_{q,j}$ are spatially-dependent weights, and $V(f_{{\rm B},q}, f_{{\rm B},j})$ is a functional which penalizes roughness in the estimated field map. For field map estimation, we choose a quadratic penalty $V(f_{{\rm B},q}, f_{{\rm B},j}) = (f_{{\rm B},q} - f_{{\rm B},j})^2$, to enforce smoothness [7], [8].

B. Optimization using network flow methods

In the VARPRO formulation, estimation of the field inhomogeneity map reduces to solving the optimization problem in Eq. 5. This is generally a very large, nonconvex, discrete problem. Typically, methods which guarantee asymptotic convergence to the global optimum (e.g., stochastic approaches [9]) are extremely slow in practice.

We focus instead on iterative descent algorithms which guarantee convergence to a local optimum with respect to very large moves (where a move consists of a set of allowed modifications to the current estimate) [10]. The final solution is reached when no improving solution can be found using the prescribed moves. The key to these methods is the design of the moves: the larger the moves, the better the solution. On the other hand, searching over a very large set may require a large amount of computation, thus making it impractical. For instance, in the case of the widely used *iterated conditional modes* (ICM) algorithm [11], voxels are updated one at a time, keeping the rest constant (i.e., the best among L candidate field maps is chosen at each step). This makes each single step very efficient, but the quality of the final solution is limited by the small size of the move.

A class of large-move search techniques for solving optimization problems of the form shown in Eq. (5) has received considerable attention in recent years. These methods are based on forming a graph such that finding a minimum cut of the graph is equivalent to minimizing the desired functional over a move of size exponential in Q, and are applicable to a wide-range of moves (which are called "graph-representable") [10], [12]. Remarkably, the equivalent minimum cut problem can be solved efficiently (requiring an amount of computation bounded by a low order polynomial in Q [13]).

In this work, we consider a broad class of moves where, given a current field map estimate $\mathbf{f}_{\rm B} = [f_{{\rm B},1}\ , \cdots ,\ f_{{\rm B},Q}]$, a second estimate $\mathbf{f}'_{\rm B} = [f'_{{\rm B},1}\ , \cdots ,\ f'_{{\rm B},Q}]$ is in the current move if, for every voxel $q = 1, \ldots, Q$, either $f'_{{\rm B},q} = f_{{\rm B},q}$ or $f'_{{\rm B},q} = g(f_{{\rm B},q}, q)$, for some predetermined function g. Thus, the move is specified by the function g. Note that the move contains 2^Q different field map estimates, many more than that of ICM for any realistic problem size. Also, note that, as opposed to voxel-by-voxel methods, any subset of the voxels can be updated simultaneously using these moves (a property which is critical for avoiding many local optima in Eq. 5). For the moves considered in this work, the necessary and sufficient condition for graph-representability is the simple requirement [12]:

$$\begin{aligned} V(f_{{\rm B},q}, f_{{\rm B},j}) + V(g(f_{{\rm B},q},q), g(f_{{\rm B},j},j)) \leq \\ V(g(f_{{\rm B},q},q), f_{{\rm B},j}) + V(f_{{\rm B},q}, g(f_{{\rm B},j},j)) \end{aligned} \tag{6}$$

for all q, j, $f_{{\rm B},q}$ and $f_{{\rm B},j}$.

A choice of g which is applicable to the present problem is the jump move, where $g(f_{{\rm B},q}, q) = f_{{\rm B},q} + \beta$ [14], [15]. Note that the size of the jump is constant over all the voxels.

While the jump move provides a powerful tool for field map estimation, it does not take into account the fact that, for most voxels, the field map estimate will be close to a local minimizer of the residual R. Here we introduce a second type of move, termed *jumpmin*, which is adapted for each voxel by moving to the next (or previous) local minimum of the residual. Defining $\{f_{{\rm B},q}^{\min,m}\}$ as the local minimizers of R at voxel q, the function g is:

$$\textit{jumpmin-next:}\ g(f_{{\rm B},q}, q) = \min_{m} f_{{\rm B},q}^{\min,m} \ \text{s.t.}\ f_{{\rm B},q}^{\min,m} > f_{{\rm B},q} \tag{7}$$

$$\textit{jumpmin-prev:}\ g(f_{{\rm B},q}, q) = \max_{m} f_{{\rm B},q}^{\min,m} \ \text{s.t.}\ f_{{\rm B},q}^{\min,m} < f_{{\rm B},q} \tag{8}$$

where $f_{{\rm B},q}$ is the current field map estimate at voxel q. The graph-representability of both the *jump* and *jumpmin* moves for a quadratic penalty V can easily be proved using Eq. 6 (the proof is omitted here due to space considerations.) The proposed *jumpmin* moves are shown graphically in Fig. 1. The details on forming the equivalent graph for the moves considered in this paper are provided in Ref. [12].

In this work, we employ a randomized scheduling of the proposed moves, where, at each iteration, either a *jump* move (with random step size) or *jumpmin* move (with random direction) is performed. At the beginning of the iteration,

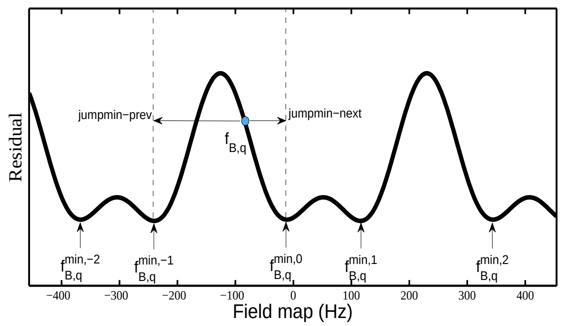

Fig. 1. Example of residual R at an individual voxel, and corresponding *jumpmin* moves.

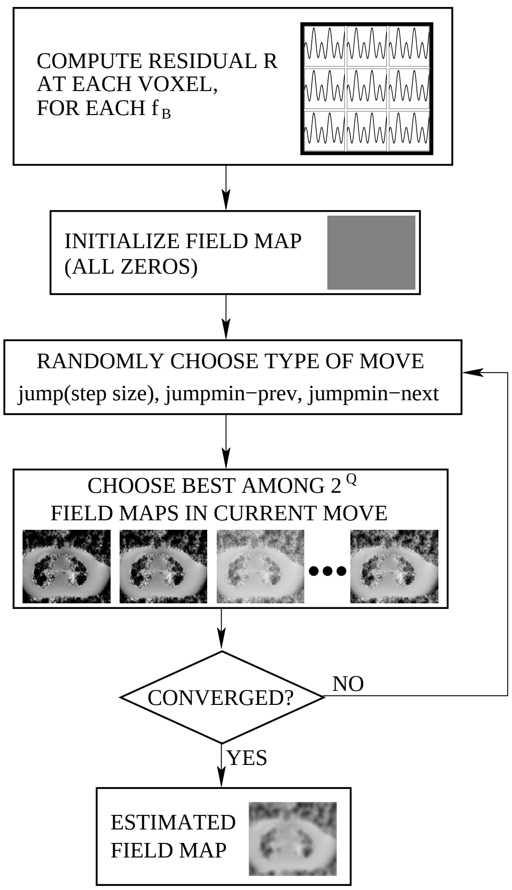

Fig. 2. Proposed field map estimation algorithm. In the core of the algorithm (choosing the best among 2^Q candidate field maps at each step), the "best" field map is the one minimizing Eq. 5.

the field map is set to all zeros. The complete algorithm is shown in Fig. 2.

III. Results and Discussion

We have tested the proposed method in a cardiac water/fat separation application, which has recently been proposed as a method to detect fibrofatty infiltration in the myocardium [16]. Cardiac imaging is particularly demanding in terms of rapid field map estimation due to the presence of tissue-air interfaces between heart and lung as well as coronary stents and sternal wires. In this application, estimating the water/fat images reduces to solving a linear least squares (LLS) problem at each voxel (finding ρ_W and ρ_F in Eq. 1), once the field map is known. Errors in the field map estimate lead to incorrect water/fat decompositions, with possible swapping of the two components.

Data were acquired on a Siemens ESPREE 1.5 T scanner using a multi-echo GRE sequence. Figure 3(a)-(c) shows results from a cardiac acquisition with echo times $\{1.6, 3.9, 6.2\}$ ms. Note the large field inhomogeneity variation observed at the edges of the field of view (due to the short, wide bore scanner). Figure 3(d)-(f) shows (for comparison) results from the same dataset using our own implementation of a previously proposed method, termed IDEAL [5]. Figure 4 shows results from a sagittal acquisition with echo times $\{4.2, 6.7, 9.2\}$ ms. For both datasets, the MRF neighborhood consisted of the 8 surrounding voxels, and the MRF weights $w_{q,j}$ were set to the energy of the signal at each location [7]. The algorithm was stopped after 50 iterations. In both cases, uniformly good water/fat separation is achieved, due to the accuracy of the field map estimates.

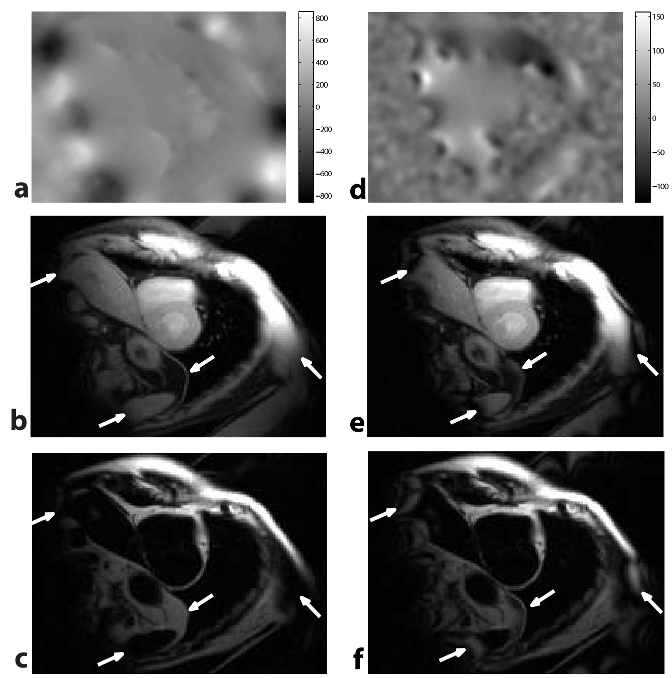

Fig. 3. (a)-(c) Results from proposed method in a cardiac water/fat separation application. (a) Estimated field map (in Hz). (b) Resulting water image. (c) Resulting fat image. (d)-(f) Shown for comparison are the results of a previously proposed method (IDEAL) [5]. Note the improved performance of the proposed method in regions of high field inhomogeneity, where IDEAL produces erroneous water/fat decompositions (see arrows in (e)).

In practice, the improved performance of the proposed method is largely due to the above described *jumpmin* moves. These moves allow rapid convergence to a good estimate because they are tailored to each voxel (as opposed to other types of moves, which are generic). However, the proposed

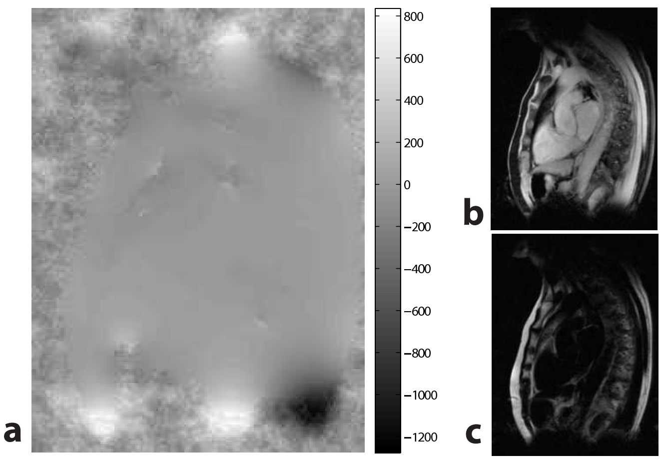

Fig. 4. Results from proposed method in a water/fat separation application (sagittal view). (a) Estimated field map (in Hz). (b) Resulting water image. (c) Resulting fat image.

algorithm also includes the standard *jump* move, which allows a smoother field map estimate in noisy regions.

In the proposed algorithm (Fig. 2), the bulk of the computation time is spent solving the network flow problem for choosing the best candidate field map at each iteration. On an Intel Xeon-based desktop PC with 8 GB of RAM and a 3.67 GHz CPU, solving this problem at each iteration requires 0.3 s for images of size 192×144, and 0.9 s for images of size 192×256 (image sizes from the results shown in this paper). Since a moderate number of iterations suffices to produce good results, these computation times are acceptable in many applications.

Perhaps surprisingly, Eq. 5 (in its discretized version) can be solved exactly in polynomial time using network flow methods. As shown in Ref. [17], this can be achieved by constructing the appropriate graph and finding a minimum cut. This result holds as long as the regularization functional $V(f_{\mathrm{B},q}, f_{\mathrm{B},j})$ is convex, even if the residual R is a nonconvex function of f_{B}, as is the case for field map estimation. Direct application of the method proposed in Ref. [17] to Eq. (5) requires the manipulation of a very large graph (containing on the order of QL^2 edges if V is quadratic), making it impractical for the problem sizes we consider. However, we can use it to efficiently compute an initial low-resolution field map estimate (e.g., size 64×64) obtained by globally minimizing Eq. 5 with ℓ_1 penalty $V(f_{\mathrm{B},q}, f_{\mathrm{B},j}) = |f_{\mathrm{B},q} - f_{\mathrm{B},j}|$ (this choice of V requires only on the order of QL edges in the equivalent graph). This low-resolution estimate provides an improved initialization (instead of all zeros) for the proposed algorithm (see Fig. 2).

For simplicity, in this paper we have focused on the case where two signal components (water and fat) are present. However, the proposed method can naturally account for more components (e.g., silicone), and can be used in the presence of only water [7], [18]. Similarly, the proposed method has been extended to include T_2^* decay [19].

IV. Conclusions

We have introduced a novel formulation for regularized field map estimation in MRI. The proposed method should prove useful in many challenging applications where a high field inhomogeneity is present.

This paper also describes an improved optimization approach based on VARPRO and network flow algorithms, which may have application for the regularized estimation of other nonlinear parameters in different imaging scenarios.

V. Acknowledgements

We acknowledge the use of the Matlab Boost Graph Library (MatlabBGL) package, written by David Gleich.

References

[1] G. Glover and E. Schneider, “Three-point Dixon technique for true water/fat decomposition with B_0 inhomogeneity correction,” *Magn Reson Med*, vol. 18, pp. 371–383, 1991.
[2] D. Noll, C. Meyer, J. Pauly, D. Nishimura, and A. Macovski, “A homogeneity correction method for magnetic resonance imaging with time-varying gradients,” *IEEE Trans Med Imaging*, vol. 10, pp. 629–637, 1991.
[3] S. Kanayamay, S. Kuhara, and K. Satoh, “In vivo rapid magnetic field measurement and shimming using single scan differential phase mapping,” *Magn Reson Med*, vol. 36, pp. 637–642, 1996.
[4] M. Bernstein, K. King, and X. Zhou, *Handbook of MRI pulse sequences*. Academic Press, September 2004.
[5] S. Reeder, Z. Wen, H. Yu, A. Pineda, G. Gold, M. Markl, and N. Pelc, “Multicoil Dixon chemical species separation with an iterative least squares estimation method,” *Magn Reson Med*, vol. 51, pp. 35–45, 2004.
[6] H. Yu, S. Reeder, A. Shimakawa, J. Brittain, and N. Pelc, “Field map estimation with a region growing scheme for iterative 3-point water-fat decomposition,” *Magn Reson Med*, vol. 54, pp. 1032–1039, 2005.
[7] J. Fessler, D. Yao, and D. Noll, “Regularized fieldmap estimation in MRI,” in *Proceedings of the 3rd IEEE International Symposium on Biomedical Imaging: Macro to Nano*, Arlington, VA, USA, 2006, pp. 706–709.
[8] D. Hernando, J. Haldar, B. Sutton, J. Ma, P. Kellman, and Z.-P. Liang, “Joint estimation of water/fat images and field inhomogeneity map,” *Magn Reson Med*, vol. 59, pp. 571–580, 2008.
[9] S. Geman and D. Geman, “Stochastic relaxation, Gibbs distributions and the Bayesian restoration of images,” *IEEE Trans Pattern Anal Mach Intell*, vol. 6, pp. 712–741, 1984.
[10] Y. Boykov, O. Veksler, and R. Zabih, “Fast approximate energy minimization via graph cuts,” *IEEE Trans Pattern Anal Machine Intell*, vol. 23, no. 11, pp. 1222–1239, November 2001.
[11] J. Besag, “On the statistical analysis of dirty pictures,” *J R Stat Soc Ser B*, vol. 48, pp. 259–302, 1986.
[12] V. Kolmogorov and R. Zabih, “What energy functions can be minimized via graph cuts?” *IEEE Trans Pattern Anal Machine Intell*, vol. 26, no. 2, pp. 147–159, 2004.
[13] T. Cormen, C. Leiserson, R. Rivest, and C. Stein, *Introduction to Algorithms*, 2nd ed. The MIT Press, 2001.
[14] O. Veksler, “Efficient graph-based energy minimization methods in computer vision,” Ph.D. dissertation, Cornell University, 1999.
[15] J. Bioucas-Dias and G. Valadao, “Phase unwrapping via graph cuts,” *IEEE Trans Image Proc*, vol. 16, no. 3, pp. 698–709, March 2007.
[16] P. Kellman, D. Hernando, S. Shah, S. Zuehlsdorff, R. Jerecic, C. Mancini, Z.-P. Liang, and A. Arai, “Multi-echo Dixon Fat and Water Separation Method for Detecting Fibro-fatty Infiltration in the Myocardium,” *Magn Reson Med*, 2008, in press.
[17] H. Ishikawa, “Exact Optimization for Markov Random Fields with Convex Priors,” *IEEE Trans Pattern Anal Machine Intell*, vol. 25, no. 10, pp. 1333–1336, 2003.
[18] B. Sutton, D. Noll, and J. Fessler, “Dynamic field map estimation using a spiral-in/spiral-out acquisition,” *Magn Reson Med*, vol. 51, pp. 1194–1204, 2004.
[19] D. Hernando, P. Kellman, J. Haldar, and Z.-P. Liang, “Estimation of water/fat images, B0 field map and T2* map using VARPRO,” in *Proceedings of ISMRM*, Toronto, 2008, in press.